

Exosomal PD-L1 promotes the formation of an immunosuppressive microenvironment in gastric diffuse large B-cell lymphoma

HUI ZENG¹, JINFENG WANG², BIAOMING XU¹, HONGYU DENG², MINGJING PENG², RILIN DENG³, SONG SHANG², QI HU¹, JUNJUN LI², JINGUAN LIN², HAIZHEN ZHU^{2,3}, YAJUN LI² and CHAOHUI ZUO¹⁻³

¹Graduates Collaborative Training Base of Hunan Cancer Hospital,

University of South China; ²Department of Gastroduodenal and Pancreatic Surgery,

Translational Medicine Research Center of Liver Cancer, Laboratory of Digestive Oncology,

The Affiliated Cancer Hospital of Xiangya School of Medicine & Hunan Cancer Hospital, Hunan Cancer Institute, Central South University, Changsha, Hunan 410013; ³Institute of Pathogen Biology and Immunology of College of Biology, Hunan Provincial Key Laboratory of Medical Virology, State Key Laboratory of Chemo/Biosensing and Chemometrics, Hunan University, Changsha, Hunan 410082, P.R. China

Received November 12, 2022; Accepted February 10, 2023

DOI: 10.3892/or.2023.8525

Abstract. Gastric diffuse large B-cell lymphoma (GDLBCL) is a common disease with an increasing incidence. However, the regulatory effect of exosomal programmed death-ligand 1 (PD-L1) on the immune microenvironment in GDLBCL is unclear. In the present study, the protein expression levels of exosomal PD-L1 in the supernatants of cultured diffuse large B-cell lymphoma (DLBCL) cells and the plasma of patients with GDLBCL was assessed using immunoblotting. Exosomes derived from DLBCL cells were cocultured with

T lymphocytes or injected into tumor xenograft mice by tail vein injection. The relationship between the protein expression level of exosomal PD-L1 in the plasma and the clinical characteristics and immune microenvironmental parameters of GDLBCL was evaluated using immunoblotting and immunohistochemistry. High levels of exosomal PD-L1 were found in the supernatants of cultured DLBCL cells. Exosomes with high levels of PD-L1 promoted growth of tumors formed by DLBCL cells *in vivo* and inhibited the proliferation of T lymphocytes. Notably, the protein expression level of PD-L1 in plasma exosomes derived from GDLBCL patients was significantly higher than that of healthy individuals. High levels of PD-L1 in plasma exosomes were significantly associated with international prognostic index score, pathological type and advanced Lugano stage, which might lead to the poor prognosis of GDLBCL. Moreover, a high level of PD-L1 in plasma exosomes was significantly associated with an immunosuppressive microenvironment in GDLBCL. Therefore, the results of the present study indicated that exosomal PD-L1 inhibited the proliferation of T lymphocytes and promoted the formation of an immunosuppressive microenvironment in GDLBCL. High expression of exosomal PD-L1 may suggest a poor prognosis of GDLBCL, and exosomal PD-L1 in plasma may be a new diagnostic indicator for GDLBCL.

Correspondence to: Professor Yajun Li or Professor Chaohui Zuo, Department of Gastroduodenal and Pancreatic Surgery, Translational Medicine Research Center of Liver Cancer, Laboratory of Digestive Oncology, The Affiliated Cancer Hospital of Xiangya School of Medicine & Hunan Cancer Hospital, Hunan Cancer Institute, Central South University, 283 Tongzipo Road, Changsha, Hunan 410013, P.R. China

E-mail: liyajun2391@163.com

E-mail: zuochaohui@vip.sina.com

Abbreviations: PGL, primary gastric lymphoma; GDLBCL, gastric diffuse large B-cell lymphoma; DLBCL, diffuse large B-cell lymphoma; NTA, nanoparticle tracking analysis; TEM, transmission electron microscope; IPI, international prognostic index; IHC, Immunohistochemistry; PD-L1, programmed death-ligand 1; NK, natural killer; R-CHOP, rituximab, cyclophosphamide, doxorubicin, vincristine, and prednisolone; CD9, cluster of differentiation 9; CD63, cluster of differentiation 63; GCB, germinal center B-cell like lymphoma

Key words: exosomes, PD-L1, gastric diffuse large B-cell lymphoma, immune microenvironment, immunosuppression

Introduction

Primary gastric lymphoma (PGL) is the most common type of extranodal tissue lymphoma of non-Hodgkin's lymphoma, accounting for 30-40% of all extranodal tissue lymphomas worldwide (1). Furthermore, PGL accounts for 4-20% of all non-Hodgkin's lymphomas and ~5% of primary gastric cancers (2). Gastric diffuse large B-cell lymphoma (GDLBCL) is the most common type of PGL and has an increasing incidence (3). Currently, chemotherapy is the main method applied

for GDLBCL therapy (4). However, GDLBCL is prone to metastasis and recurrence (5). Evaluation of the pathology of GDLBCL and development of effective therapeutic methods are urgently needed.

Immunotherapy reverses the immunosuppression induced by cancer, which enhances the killing effect of immune cells toward cancer cells. Because they enhance the anticancer effect of adaptive immunity based on effector T cells, inhibitors of immune checkpoints are widely used in cancer treatment, which has opened a new era for immunotherapy (6,7). Although programmed cell death protein 1 (PD-1) and programmed death-ligand 1 (PD-L1) inhibitors have sustained anticancer effects in certain neoplastic cases, most patients do not benefit from immunotherapy due to the heterogeneity of immune responses and cancer (8-10). The upregulated expression of PD-L1 is significantly associated with poor survival in DLBCL (11). Our previous study reported the suppressive effect of the innate immune effector ISG12a on the transcriptional activity of PD-L1, which indicated the inhibitory effect of the PD-L1/PD-1 axis on natural killer (NK) cell-mediated anticancer immunity (12). Moreover, we previously reported that PD-L1 is a prognostic factor for primary GDLBCL patients treated with rituximab, cyclophosphamide, doxorubicin, vincristine, and prednisolone (R-CHOP) (13). However, the regulatory effect of PD-L1 on GDLBCL is still unclear.

Exosomes are a type of membranous vesicle with a diameter of 40-200 nm with special expression of protein markers such as cluster of differentiation 9 (CD9), cluster of differentiation 63 (CD63), and tumor susceptibility gene 101 protein (14,15). Exosomes carry biologically active molecules such as RNA and protein, transmitting signals between cells and influencing the extracellular environment and cancer biology (16,17). Cancer-derived extracellular vesicles have been reported to be promising therapeutic targets and disease biomarkers (18,19). Specifically, exosomal PD-L1 may downregulate CD69 expression by effector T cells in HNSCC, suppress the function of CD8 T cell reinvigoration in cancers, such as melanoma, and inhibit CD8+ T cell proliferation and activation in colon cancer, which influences the therapeutic efficiency of clinical cancer (20-22). Interestingly, DLBCL-derived exosomes induce apoptosis and upregulation of PD-1 in T cells *in vitro*; however, dendritic cells (DCs) pulsed DLBCL-derived exosomes stimulate the anti-lymphoma potency of T cells *in vivo* (23). It is important to elucidate the regulatory role and mechanism of exosomal PD-L1 in GDLBCL.

Cell-intrinsic PD-L1 promotes the occurrence and development of GDLBCL; however, the regulatory effect of exosomal PD-L1 derived from GDLBCL cells on the immune microenvironment is still unclear. Although T cells, natural killer (NK) cells, macrophages and other immune cells are involved in the formation of the tumor microenvironment, immuno-oncology, represented by the inhibitory PD1/PD-L1 signaling, is mainly focused on enhancing T-cell responses (24). Specifically, myriad intricate regulatory mechanisms control T cell function in the context of anti-tumor immunity (25). Interestingly, the CAR-T therapy for GDLBCL has been performed globally with promising results (26,27). It is of great clinical significance to evaluate the regulatory relationship between T cells and GDLBCL. In the present study, the regulatory role of exosomes derived

from DLBCL cells with high levels of PD-L1 were evaluated in tumor growth and T-cell proliferation.

Materials and methods

Cell culture. The DLBCL cell lines U2932 (RRID: CVCL_1896) and OCI-LY8 (RRID: CVCL_8803) were purchased from Nanjing Cobioer Biotechnology Co., Ltd., the human gastric mucosal epithelial cell line GES-1 (RRID: CVCL_EQ22) was kindly provided by the Institute of Oncology, Nanhua University (Hengyang, China), and the human T cell line H9 (RRID: CVCL_1240) was purchased from Shanghai Yiyan Biotechnology Co., Ltd. U2932, OCI-LY8 and H9 cells were cultured in RPMI 1640 medium (Thermo Fisher Scientific, Inc.) with 10% (v/v) heat inactivated fetal bovine serum (FBS; Thermo Fisher Scientific, Inc.), 100 units/ml penicillin (Thermo Fisher Scientific, Inc.) and 100 μ g/ml streptomycin (Thermo Fisher Scientific, Inc.). H9 cells were cultured in 75 cm² tissue culture flasks at 37°C in an incubator with 5% CO₂ and 95% humidity, and the culture medium was refreshed every 2-4 days. H9 cells were centrifuged at 125 x g at room temperature for 5-10 min and resuspended in fresh medium at 5x10⁵ cells/ml to remove cell debris and replace the medium. For good growth states, H9 cells were maintained at cell concentrations between 5x10⁵ and 2x10⁶ cells/ml. Passage of U2932 and OCI-LY8 cells was performed when cells reached 80-90% confluence. U2932 and OCI-LY8 cells were sequentially centrifuged at 125 x g at room temperature for 5 min, resuspended in 2 ml fresh medium, seeded into a new 25 cm² cell culture bottle with 8 ml fresh culture medium. The human normal gastric mucosal GES-1 cell line was cultured in Dulbecco's modified Eagle's medium (Thermo Fisher Scientific, Inc.) with 10% (v/v) FBS, 100 U/ml penicillin (Thermo Fisher Scientific, Inc.) and 100 μ g/ml streptomycin (Thermo Fisher Scientific, Inc.). The FBS used for cultivation of all types of cells was ultracentrifuged at 100,000 x g and 4°C for 10 h to remove exosomes. All kinds of cells were cultured at 37°C in a cell incubator with 5% CO₂.

Plasmid construction. The total cellular RNA isolated using TRIzol[®] reagent (Thermo Fisher Scientific, Inc.) from U2932 cells was used for synthesis of complementary DNA using the PrimeScript[™] RT reagent Kit with gDNA Eraser (Takara Biotechnology Co., Ltd.). Sequences used for plasmid construction were obtained using a high-fidelity PCR kit KOD-Plus-Neo (Toyobo Life Science) and cloned into the p3xFlag-CMV-14 vector (MilliporeSigma). The primers used for plasmid construction were as follows: forward, 5'-GGGGTACCATGAGGATATTTGCTGTCTTT-3' and reverse, 5'-GCTCTAGACGTCTCCTCCAAATGTGTA GT-3'. Gene silencing plasmids for PD-L1 were constructed using the pRNAT-U6.1/neo vector (GenScript) according to the manufacturer's protocols. The target sequence used for constructing the gene silencing plasmid shRNA-PD-L1 was 5'-GCATTTGCTGAACGCATTT-3'. The negative control (target sequence: 5'-ACTACCGTTGTTATAGGTG-3') was constructed previously (12). All plasmids were amplified using *Escherichia coli* DH5 α competent cells and were sequenced by Sangon Biotech Co., Ltd to confirm the correct construction of the plasmid.

Cell transfection of plasmids. Cell transfection of plasmids was performed according to the manufacturer's protocols. Briefly, a total of 1.5×10^6 cells at the logarithmic growth stage were seeded into each well of a 12-well cell culture plate. A total of 1 μ g plasmids and 4 μ l Lipofectamine[®] 2000 (Thermo Fisher Scientific, Inc.) were mixed in 100 μ l of Opti-MEM[™] medium (Thermo Fisher Scientific, Inc.), separately. After incubation for 5 min at room temperature, plasmids and Lipofectamine[®] 2000 were mixed together and incubated at room temperature for 20 min. Then, 200 μ l of the mixture was added to each well of the 12-well cell culture plate. After transfection at 37°C for 12 h, the culture medium was replaced with fresh medium. The cells were used for further experiments 24–48 h after transfection.

Extraction and characterization of exosomes. Exosomes in the supernatants of cultured cells were extracted by ultracentrifugation according to previously reported protocols (28). Briefly, the supernatants of cultured cells were centrifuged at 2,000 x g and 4°C for 20 min and then transferred into a centrifuge tube. The supernatants were then centrifuged at 10,000 x g and 4°C for 30 min and then transferred into new ultracentrifuge tubes. The supernatants were then ultracentrifuged at 100,000 x g and 4°C for 70 min, and the remaining supernatants were discarded. The pellets were resuspended in PBS and ultracentrifuged at 100,000 x g and 4°C for 70 min. The pellets were considered to be the extracted exosomes, which were resuspended in PBS or RIPA lysis buffer (Thermo Fisher Scientific, Inc.) with proteinase inhibitors. Exosomes in the plasma of GDLBCL patients and healthy individuals were extracted using the Exoquick TC kit (System Biosciences, LLC) according to the manufacturer's protocols. The extracted exosomes were identified by nanoparticle tracking analysis (NTA) and transmission electron microscopy (TEM) as previously reported (29). Protein expression levels of specific markers of exosomes, CD9 and CD63, were assessed using immunoblotting.

Immunoblotting. The DLBCL cells were lysed using RIPA lysis buffer (Thermo Fisher Scientific, Inc.) with proteinase inhibitors. After incubation on ice for 15–30 min, lysates were centrifuged at 16,100 x g and 4°C for 15 min. After determination of the protein concentration by the BCA method, 40 μ g total protein was sequentially run on 10% SDS-PAGE gels and transferred onto PVDF membranes which were blocked with 5% skim milk at room temperature for 1 h. Membranes were incubated with the primary antibodies at 4°C overnight, washed using TBST buffer with 1% Tween-20, and incubated with the secondary antibodies at room temperature for 2 h. Protein bands were detected using the SuperSignal[®] West Pico Chemiluminescent Substrate kit (Thermo Fisher Scientific, Inc.). β -actin was used as the internal control for total protein, and CD9 and CD63 were used as the internal controls for exosomes. Densitometric analysis of protein bands was performed using software Image Lab (version 5.2; Bio-Rad Laboratories, Inc.). The antibodies used in the present study were as follows: Rabbit anti-PD-L1 (1:1,000, clone E1L3N, cat. no. 13684, Cell Signaling Technology, Inc.), mouse anti- β -actin (1:5,000, clone AC-15, A5441, Sigma-Aldrich; Merck KGaA), mouse anti-Flag (1:5,000, clone M2, F3165,

MilliporeSigma), mouse anti-CD9 (1:200, clone C-4, sc-13118, Santa Cruz Biotechnology, Inc.), mouse anti-CD63 (1:200, clone MX-49.129.5, cat. no. sc-5275, Santa Cruz Biotechnology, Inc.), goat anti-mouse IgG (HRP-linked, 1:5,000, AP124P, MilliporeSigma), goat anti-rabbit IgG (HRP-linked, 1:5,000, AP132P, MilliporeSigma).

MTT assay. Briefly, an average of 1×10^4 stably transfected DLBCL cells in 100 μ l of culture medium were seeded per well of a 96-well cell culture plate. After culturing at 37°C for 24 h, 10 μ l of 5 mg/ml MTT solution was added to the culture medium and incubated at 37°C for 4 h. Then, the culture medium was carefully removed and replaced with 150 μ l of DMSO. The OD value at 490 nm was quantified using a Synergy HTX microplate reader (BioTek Instruments, Inc.). Experiments were repeated three times.

Animal experiment. A total of 12 NOD-SCID mice (age, 6 weeks; average weight, 20 g; Hunan Slack Jingda Experimental Animal Co., Ltd.) were used to perform animal experiments. Mice were fed under standard conditions (25°C and 50% humidity) with free access to sterile feed and water in a pathogen-free environment with a 12 h light/dark cycle at the animal care facility of Hunan Cancer Hospital (Changsha, Hunan, China). The mice were randomly assigned to two groups with six mice per group. An average of 5×10^6 U2932 cells in 200 μ l of sterile PBS were subcutaneously injected into all mice. Seven days after cell injection, 100 μ g of exosomes derived from U2932 cells stably transfected with the p3xFlag vector or p3xFlag-PD-L1 in 100 μ l of sterile PBS were administered to the mice every four days through the tail vein. Mice were sacrificed when they experienced a sharp decrease in activity, water and diet intake, if the tumors formed under the skin of mice were assessed to be about to reach 15 mm in diameter in any dimension or if a total of 30 days after cell injection was reached. The mice were sacrificed by cervical dislocation immediately after isoflurane anesthesia (induction, 3%; maintenance, 1%). The formed tumors were measured every two days and recorded for further analysis.

Clinical specimens. All tissue specimens used in the present study were obtained from Hunan Cancer Hospital with the informed consent of patients and the present study was approved by the institutional review boards of Hunan Cancer Hospital (approval no. 2021-012) and was performed in accordance with the Declaration of Helsinki. The blood samples of 26 GDLBCL patients were collected from Hunan Cancer Hospital from January 2017 to December 2020. The inclusion criteria used were as follows: i) the stomach was the primary site, which may have been accompanied by lymph node metastasis in the gastric drainage area; and ii) the pathological diagnosis was DLBCL. Samples that failed to meet both of the above inclusion criteria were excluded. A total of 10 males and 16 females, aged 30–69 years old with a median age of 51.2 years were included. The patients were not treated with antineoplastic therapy before samples were taken. The Lugano stage (2016) (30) of patients was stages I–II in 15 cases and stages III–IV in 11 cases. The international prognostic index (IPI) score (31) of the lymphomas was 0–2 in 16 cases and 3–5 in 10 cases. The histological

classification was 14 cases in the non-germinal center B-cell like lymphoma (non-GCB) subtype and 12 cases in the GCB subtype. A total of 22 healthy individuals who volunteered in the same period were selected as the normal control group, which included 10 males and 12 females (median age, 48.5 years; age range, 26-62 years).

Immunohistochemistry (IHC). Tissue sections used for IHC were assessed by two pathologists at Hunan Cancer Hospital (Changsha, Hunan, China), and IHC staining was performed as previously reported (12). Briefly, fresh tissues collected immediately after surgery were routinely fixed using 10% formalin solution at room temperature for 24 h, embedded in paraffin, followed by slicing into 5 μ m sections. Then, tissue sections were dewaxed in xylene at room temperature and rehydrated in graded alcohols, and tissue antigen retrieval was performed in boiled 1 μ M sodium citrate solution (pH, 6.0) at 100°C for 2 min. After blocking with normal goat serum (Thermo Fisher Scientific, Inc.) at room temperature for 1 h, slices were sequentially incubated with the primary antibodies at 4°C overnight and secondary antibodies for 2 h at room temperature, stained with DAB solution at room temperature for 5 min, and counterstained with hematoxylin at room temperature for 1 min. The antibodies used for IHC staining were as follows: Rabbit anti-PD-1 (1:200, clone D4W2J, cat. no. 86163S, Cell Signaling Technologies, Inc.), rabbit anti-PD-L1 (1:500, 17952-1-AP, Proteintech Group, Inc.), mouse anti-CD8 (1:5,000, clone 1G2B10, cat. no. 66868-1-Ig, Proteintech Group, Inc.), rabbit anti-CD5 (1:800, clone E8X3S, cat. no. 39300S, Cell Signaling Technologies, Inc.), rabbit anti-CD10 (1:500, clone E5P7S, cat. no. 65534S, Cell Signaling Technologies, Inc.), rabbit anti-CD20 (1:200, clone E7B7T, cat. no. 48750S, Cell Signaling Technologies, Inc.), rabbit anti-CD79a (1:250, clone D1X5C, cat. no. 13333S, Cell Signaling Technologies, Inc.), mouse anti-Ki67 (1:2,000, clone 8D5, cat. no. 9449S, Cell Signaling Technologies, Inc.), goat anti-mouse IgG (HRP-linked, 1:2,000, cat. no. AP124P, MilliporeSigma), and goat anti-rabbit IgG (HRP-linked, 1:2,000, cat. no. AP132P, MilliporeSigma).

Tissue slices were viewed under an inverted microscope, and representative images were presented in the figures. Three fields of view per section were analyzed. Positivity for CD5, CD10, CD8, PD-L1 and PD-1 was defined as $\geq 5\%$ positively stained cells, and positivity for CD20, CD79a and Ki67 was defined as $\geq 50\%$ positively stained cells. One-fifth of the cases were scored by two observers to assess reproducibility. For cases to be considered suitable for evaluation, $\geq 25\%$ area of a tissue slice had to be available for morphologic analysis following staining and at least one positively stained tumor-infiltrating macrophage was required as a positive internal control. Analysis of IHC staining of CD3, CD5, CD8, CD10 and CD20 was performed according to the manufacturers' protocols and as previously reported (32).

Statistical analysis. Data analysis was performed using SPSS version 22.0 (IBM, Corp.). Statistical graphs were drawn using GraphPad Prism 5.0 (GraphPad Software; Dotmatics). Unpaired, two-sided Student's t-test was used to assess the

statistical significance. The relationship between the PD-L1 level in plasma exosomes and the clinicopathological characteristics of GDLBCL patients was determined using the χ^2 or Fisher's exact test. Data were presented as the mean \pm SD from three independent biological replicates. $P < 0.05$ was considered to indicate a statistically significant difference.

Results

PD-L1 in exosomes derived from DLBCL cells promotes oncogenesis. To assess the regulatory role of exosomal PD-L1 in the immune microenvironment of GDLBCL, U2932 and OCI-LY8 DLBCL cells were chosen as experimental cell models and the supernatants of the cell culture medium were collected to extract exosomes by ultracentrifugation. The protein markers CD9 and CD63 detected using immunoblotting indicated the successful extraction of exosomes (Fig. 1A). NTA demonstrated that the particle size of exosomes in the supernatants of cultured cells presented a normal distribution and was mainly concentrated between 70 and 120 nm (Fig. 1B). Interestingly, compared with the protein expression level of exosomal PD-L1 derived from human epithelial gastric mucosal GES-1 cells, the protein expression level of PD-L1 in exosomes derived from DLBCL cells U2932 and OCI-LY8 was much higher (Fig. 1A). We hypothesized that the high protein expression level of exosomal PD-L1 might facilitate the initiation and development of GDLBCL.

Next, Flag-tagged PD-L1 was overexpressed or PD-L1 expression was silenced using shRNA gene-silencing plasmids in U2932 and OCI-LY8 cells. Assessment of the protein content using immunoblotting, demonstrated that Flag-tagged PD-L1 appeared in exosomes derived from the supernatants of U2932 and OCI-LY8 cells (Fig. 1C). Moreover, the protein expression level of exosomal PD-L1 was markedly decreased with the inhibition of cell intrinsic PD-L1 (Fig. 1D). These findings indicated that the protein expression level of exosomal PD-L1 was consistent with the protein expression level of cell-intrinsic PD-L1.

To further illustrate the regulatory role of exosomal PD-L1, tumor xenograft and tail vein injection experiments were performed in NOD-SCID mice. One week after injecting wild-type U2932 cells into mice, exosomes derived from the supernatants of U2932 cells overexpressing PD-L1 and the control vector were administered into mice through tail vein injection. Four weeks after cell injection, significantly larger and heavier tumors were observed in the mice injected with exosomes derived from PD-L1-overexpressing cells compared with that of the control (Fig. 1E). These results indicated that, exosomal PD-L1 contributed to tumor growth *in vivo*.

Exosomal PD-L1 inhibits the proliferation of T lymphocytes. As exosomal PD-L1 contributes to the immune evasion of cancer cells, it was hypothesized that exosomal PD-L1 might influence T lymphocytes in the immune microenvironment. Therefore, the influence of exosomal PD-L1 from the supernatants of cultured DLBCL cells on the proliferation of H9 human T lymphocytes was assessed. In MTT experiments, exosomes with PD-L1 overexpression or PD-L1 silencing as well as those of controls derived from U2932 and OCI-LY8 cells were added to the culture medium of H9 cells. The proliferation of H9

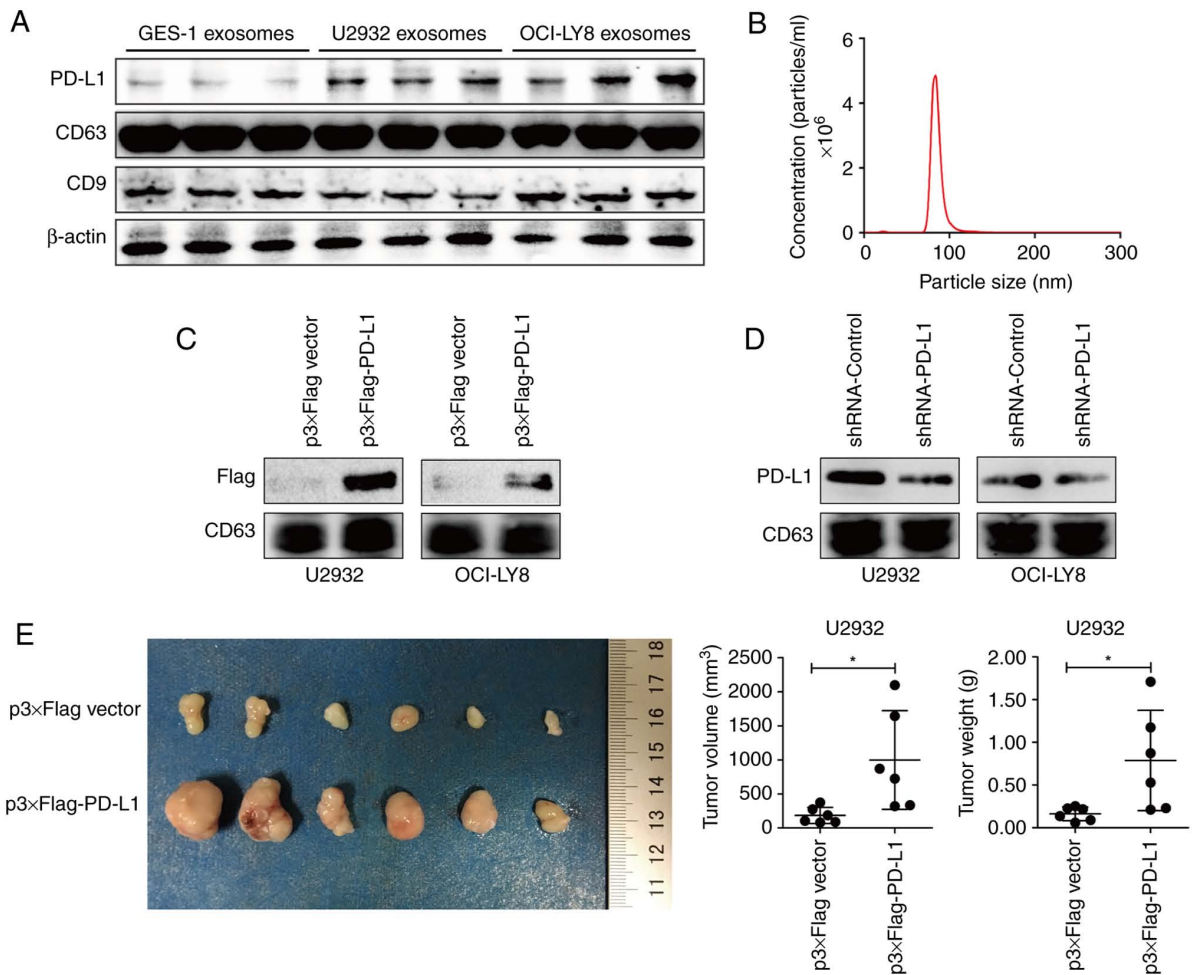


Figure 1. Influence of exosomes derived from DLBCL cells on tumor growth *in vivo*. (A) Immunoblotting for PD-L1, CD9, CD63 and β -actin in exosomes from the supernatants of cultured DLBCL U2932 and OCI-LY8 cells, and human gastric mucosal epithelial GES-1 cells. (B) NTA for the size of exosomes extracted from the supernatants of cultured U2932 cells. Immunoblotting for Flag and PD-L1 in exosomes derived from the supernatants of cultured U2932 and OCI-LY8 cells with (C) overexpression or (D) inhibition of PD-L1. (E) Tumors formed by U2932 cells in NOD-SCID mice. Data were analyzed using unpaired, two-sided Student's t-test and are presented as the mean \pm SD. * $P < 0.05$. DLBCL, diffuse large B-cell lymphoma; NTA, nanoparticle tracking analysis; shRNA, short hairpin RNA; PD-L1, programmed death-ligand 1.

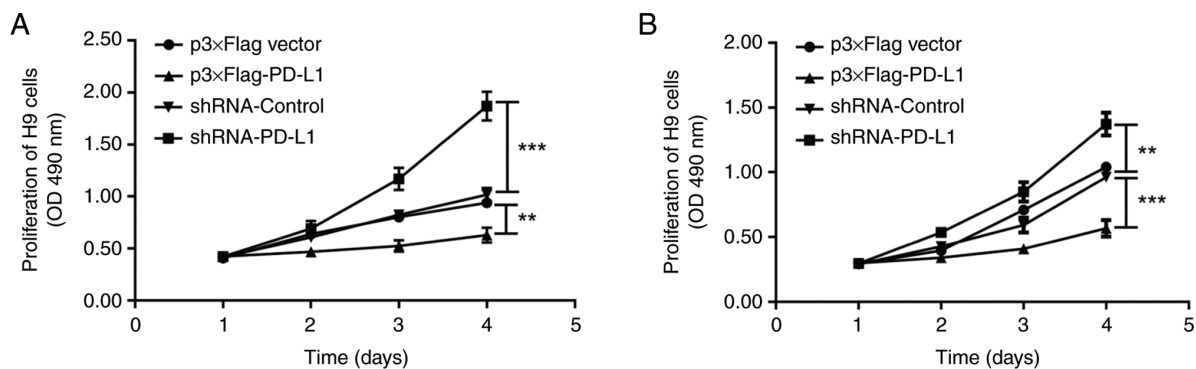


Figure 2. Regulatory effect of exosomal PD-L1 on T-cell proliferation. Proliferation of T cells influenced by exosomes derived from DLBCL (A) U2932 and (B) OCI-LY8 cells. A total of 24 h after seeding H9 cells in a 12-well cell culture plate, $2 \mu\text{g}$ of exosomes derived from DLBCL U2932 and OCI-LY8 cells with differential expression of PD-L1 were added to the supernatant of the culture medium, and the proliferation of H9 cells was then assessed using MTT assays at different time points. Data were analyzed using unpaired, two-sided Student's t-test and are presented as the mean \pm SD. ** $P < 0.01$ and *** $P < 0.001$. DLBCL, diffuse large B-cell lymphoma; shRNA, short hairpin RNA; PD-L1, programmed death-ligand 1.

cells was significantly inhibited by treatment with exosomes with PD-L1 overexpression compared with the control and was significantly promoted by treatment with exosomes with

PD-L1 silencing compared with the control (Fig. 2). These results demonstrated that PD-L1 in exosomes derived from DLBCL cells inhibited the proliferation of T lymphocytes.

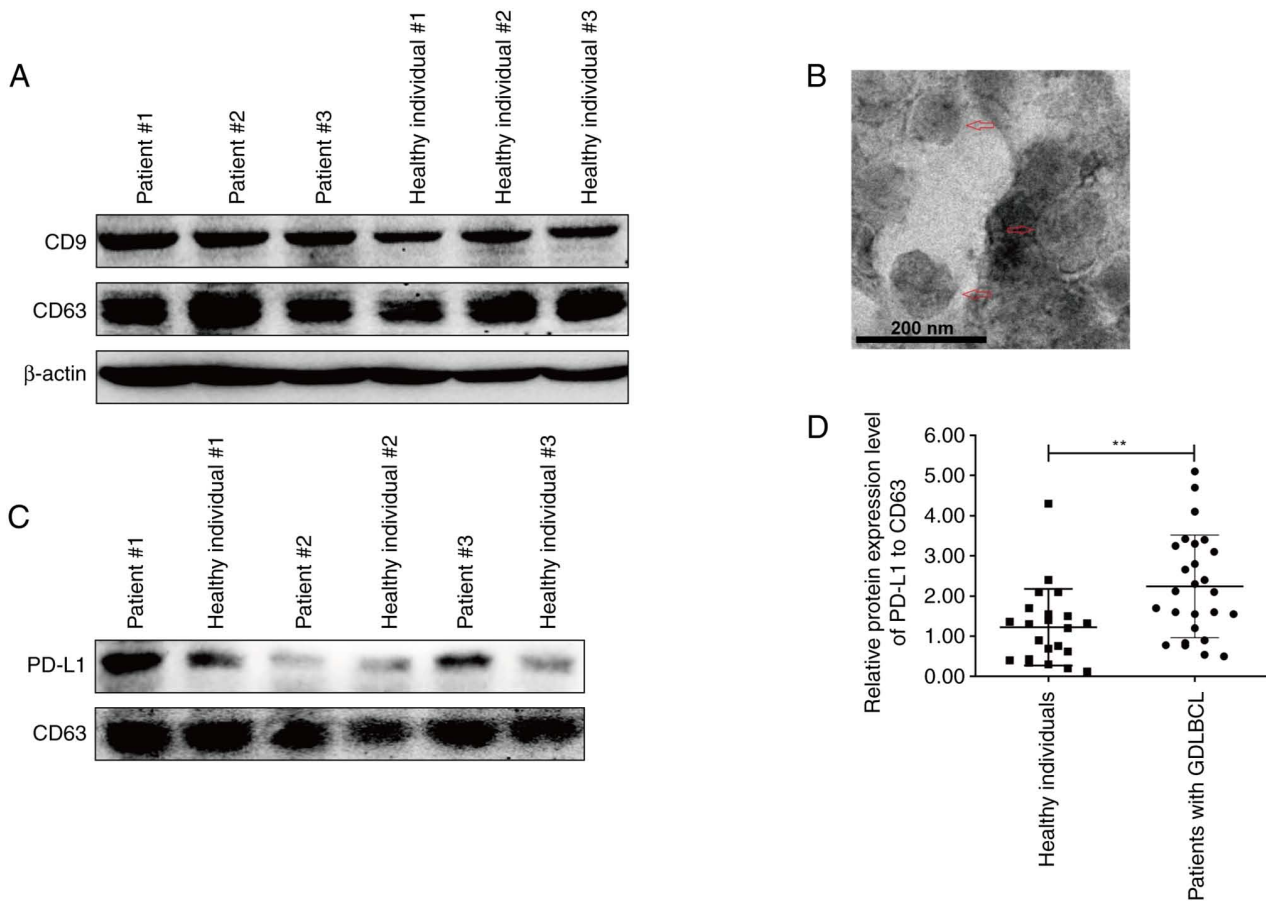


Figure 3. Differential protein expression level of PD-L1 in plasma exosomes of patients with GDLBCL and healthy individuals. (A) Immunoblotting for specific markers of exosomes, including CD9 and CD63, and β -actin. (B) Transmission electron microscopy for morphology of exosomes extracted from plasma of a representative patient with GDLBCL. Red arrows indicate the exosomes. (C) Immunoblotting for differential levels of PD-L1 protein in plasma exosomes derived from three representative patients with GDLBCL and three healthy individuals. (D) Scatter plots presenting the relative protein expression levels of PD-L1 in plasma exosomes, compared between 22 healthy individuals and 26 patients with GDLBCL. Data were analyzed using unpaired, two-sided Student's t-test and are presented as the mean \pm SD. ** $P < 0.01$. GDLBCL, gastric diffuse large B-cell lymphoma; PD-L1, programmed death-ligand 1.

Therefore, exosomal PD-L1 originating from DLBCL cells may interact with the surface PD-1 of T lymphocytes, resulting in immune suppression.

High levels of exosomal PD-L1 are associated with malignant transformation and poor prognosis in GDLBCL. Exosomes from the plasma of GDLBCL patients and healthy individuals were obtained for analysis. The detection of CD9 and CD63 proteins indicated the successful extraction of plasma exosomes (Fig. 3A). The exosomes extracted from the plasma were also assessed using TEM (Fig. 3B). Interestingly, the protein expression level of exosomal PD-L1 in three representative GDLBCL patients was markedly higher than that in healthy individuals (Fig. 3C). The statistical analysis demonstrated significant upregulation of exosomal PD-L1 in the plasma of GDLBCL patients (Fig. 3D). These data indicated that exosomes with high levels of PD-L1 may participate in the occurrence and development of GDLBCL.

The correlation between the protein expression level of exosomal PD-L1 and clinicopathological features of GDLBCL was further analyzed, including gender, age, Lugano stage, IPI score and pathological subtypes of lymphoma (Table I). Although no significant relationship was demonstrated between the protein expression level of exosomal PD-L1

in plasma and gender or age, the protein expression level of exosomal PD-L1 was demonstrated to be significantly, positively related with the IPI score, non-GCB pathological type or Lugano stage of GDLBCL. These results indicated that a high level of exosomal PD-L1 may lead to malignant transformation and poor prognosis of GDLBCL.

A high level of exosomal PD-L1 is a potential indicator of the immunosuppressive microenvironment of GDLBCL. To evaluate the relationship between exosomal PD-L1 in the plasma and the immune microenvironment of GDLBCL, the protein expression levels of CD20, CD79a, CD5, CD10, Ki67, CD8, PD-1 and PD-L1 were assessed using IHC staining in a series of consecutive slices of GDLBCL tissue specimens (Fig. 4A and B). The relationship between the protein expression level of PD-L1 in plasma exosomes and the immune microenvironment was evaluated (Table II). The protein expression levels of PD-L1 and CD8 in tissue specimens were significantly and positively related to the upregulation of PD-L1 expression in plasma exosomes ($P = 0.0004$ and $P = 0.0183$, respectively; Table II). Exosomal PD-L1 from gastric cancer cells interacts with the surface PD-1 on CD8⁺ T cells, which leads to immune evasion of cancer cells (21). Therefore, a high expression level of exosomal PD-L1 in the plasma may reflect

Table I. The relationship between the protein expression level of programmed death-ligand 1 in plasma exosomes and the clinicopathological characteristics of patients with gastric diffuse large B-cell lymphoma.

Clinicopathological characteristics	Number of patients	Exosomal PD-L1 level		P-value
		High	Low	
Gender				0.6882
Male	10	4	6	
Female	16	9	7	
Age, years				0.4110
>60	9	6	3	
≤60	17	7	10	
IPI score				0.0414
0-2	16	5	11	
3-5	10	8	2	
Pathological type				0.0183
Non-GCB	14	10	4	
GCB	12	3	9	
Lugano stage				0.0055
I + II	15	4	11	
III + IV	11	9	2	

IPI, international prognostic index; GCB, germinal center B-cell like lymphoma.

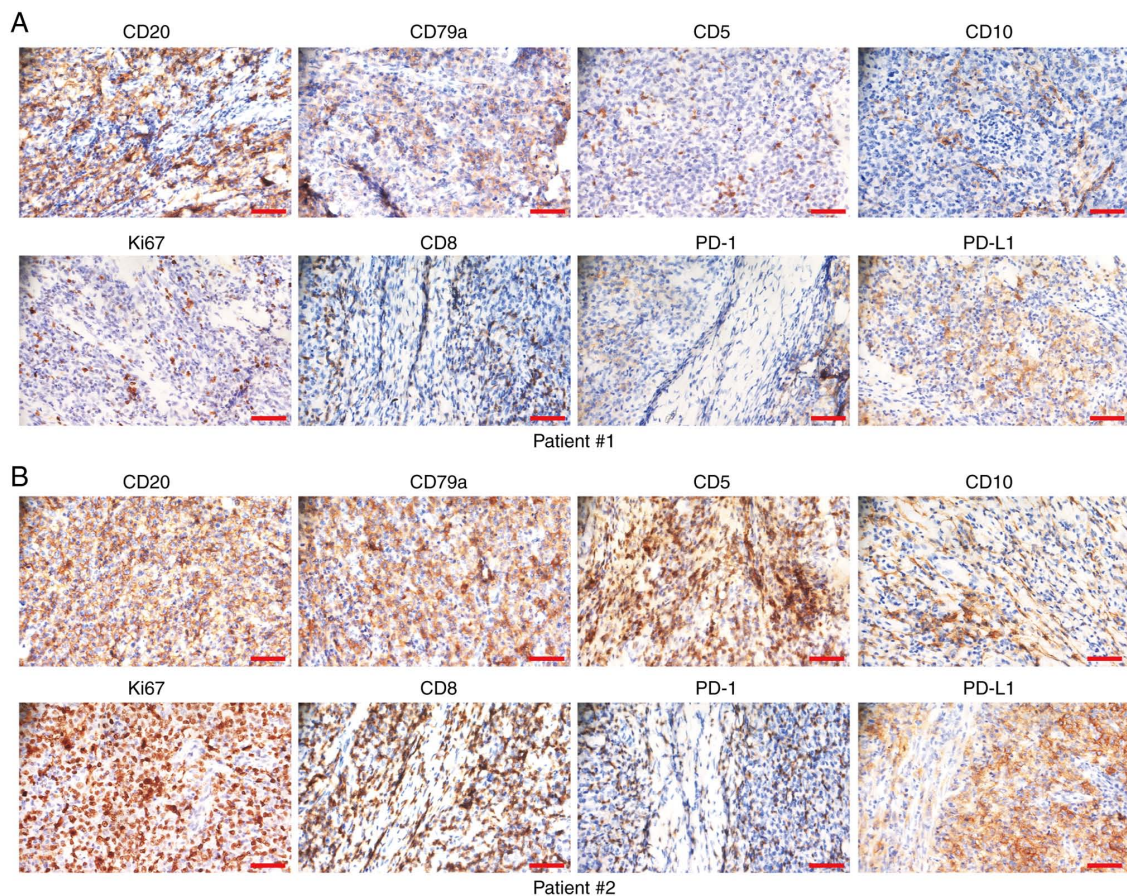


Figure 4. Protein expression levels of protein markers of B cells and the immune microenvironment in tissue specimens of gastric diffuse large B-cell lymphoma. (A and B) Immunohistochemistry images of protein expression levels of the proliferative B-cell markers CD20, CD79a, CD5, CD10, Ki67 and PD-L1 as well as the immune microenvironmental markers CD4, CD8 and PD-1 in two representative tissue specimens of GDLBCL. Scale bar=50 μm. PD-L1, programmed death-ligand 1.

Table II. The relationship between the protein level of PD-L1 in plasma exosomes and the immune microenvironment of gastric diffuse large B-cell lymphoma.

Protein level	Number of patients	Exosomal PD-L1 level		P-value
		High	Low	
CD20				>0.9999
+	21	11	10	
-	5	2	3	
CD79a				0.6447
+	20	9	11	
-	6	4	2	
CD5				>0.9999
+	3	1	2	
-	23	12	11	
CD10				0.6914
+	11	6	5	
-	15	7	8	
Ki67				0.3783
+	19	8	11	
-	7	5	2	
CD8				0.0183
+	12	9	3	
-	14	4	10	
PD-1				0.2393
+	13	5	8	
-	13	8	5	
PD-L1				0.0004
+	15	12	3	
-	11	1	10	

PD-1, programmed cell death protein 1; PD-L1, programmed death-ligand 1.

the immunosuppressive microenvironment of GDLBCL. There was no significant relationship between the protein expression level of PD-L1 in plasma exosomes and that of CD20, CD79a, CD5, CD10, Ki67 or PD-1 in GDLBCL tissue specimens (Table II).

Discussion

Immunotherapies targeting PD-1/PD-L1 have been reported to be effective strategies for the treatment of malignances (33,34). However, only 10-30% of patients have a persistent response to PD-L1/PD-1 antibody therapy in the clinic (35), which may be partly caused by the heterogeneity of the tumor microenvironment (36,37). In the present study, it was demonstrated that the exosomal PD-L1 of DLBCL cells promoted tumor growth *in vivo* and inhibited the proliferation of T lymphocytes *in vitro*. The PD-L1 protein expression level in plasma exosomes was significantly correlated with the positive rate of PD-L1 and CD8 in GDLBCL tissue. Moreover, a higher level of plasma exosome PD-L1 was demonstrated to be significantly related to patients with IPI scores ≥ 2 and advanced Lugano stage, which

may be linked with the poorer prognosis of GDLBCL. The tumor microenvironment induces the upregulation of PD-L1 in cancer cells, especially on the surface of aggressive B-cell lymphomas, which inhibits cytotoxic T cells by binding with the PD-1 receptor on effector T cells (38,39). Moreover, immunosuppressive lymphocytes such as regulatory T cells and myeloid-derived suppressor cells hinder the progression of the cell cycle and the proliferation of cytotoxic T cells as well as the function of T cells, and induce the depletion of T cells, which leads to immune tolerance (40,41). The downregulation of cytokines such as IFN- γ and IL-2 also aggravates peripheral immune tolerance, which leads to immune evasion by cancer cells (42).

Exosomes have lipid bilayer membrane structures, which can provide a protective barrier for vulnerable biomolecules. Based on biofunctions such as transmitting biological information through protein or RNA, exosomes have been regarded as promising drug carriers (43). Regarding the regulation of the tumor immune microenvironment, exosomes with high levels of PD-L1 inhibit T-cell activation and become a major regulator in cancer progression; moreover, inhibition of exosomal

PD-L1 can lead to persistent systemic anticancer immunity (21,44,45). In a model of anti-PD-L1 antibody resistance, removal of exosomal PD-L1 inhibited tumor growth (44). In the present study, the inhibitory effect, of exosomes with high expression of PD-L1, on the proliferation of T cells was demonstrated. Moreover, PD-L1 levels in plasma exosomes were increased with the occurrence and development of GDLBCL, which was associated with CD8 and PD-L1 staining in tumor tissues. Apart from the inhibitory effect on CD8⁺ T cells and exosomal PD-L1 also inhibits the proliferation of CD4⁺ T cells (46,47), decreases cytotoxic activity of NK cells against tumor cells (46,48), increased the secretion of IL-6, TNF- α and CCL2 by THP1 cells (49), promotes PD-L1 expression and phosphorylation of STAT3 in CD14⁺ monocytes (50), and predicts the efficacy of anti-PD-1/PD-L1 therapy (21). All these findings suggested that an immunosuppressive microenvironment was constructed by exosomes with high expression of PD-L1. However, exosomes imaged using TEM were not clear, which may have been due to the residual salt in the buffer solution of the exosome sample. Nevertheless, it was still possible to distinguish the typical saucer shape of exosomes in the TEM images from the present study. The quality of the TEM images needs to be improved in future studies.

PD-L1 is widely expressed in numerous types of lymphoma tissues and lymphoma cell lines (39,51). A previous retrospective study reported that the positive rate of PD-L1 in cancer tissues of GDLBCL was 60.6%, which was significantly correlated with advanced Lugano stage and high IPI score, as well as poor prognosis (13). Rossille *et al* (52) reported that the expression level of PD-L1 was correlated with the prognosis of DLBCL patients. Compared with patients with high plasma soluble PD-L1 levels at the initial diagnosis, the 3-year overall survival of patients with low plasma soluble PD-L1 was 76% vs. 89% ($P < 0.001$) (52). Patients with high levels of soluble PD-L1 at the time of initial diagnosis were reported to return to normal levels after achieving complete remission. In the present study, the high level of PD-L1 protein in plasma exosomes was significantly correlated with the positive rate for PD-L1 and CD8 in GDLBCL tissues. Moreover, a high level of exosomal PD-L1 in plasma was significantly associated with the non-GCB subtype and poor prognosis, which led to an IPI score ≥ 2 and advanced Lugano stage ($P < 0.05$). These findings suggested that a high level of PD-L1 in plasma exosomes may be a biomarker for the poor prognosis of GDLBCL.

Exosomal PD-L1 is positively correlated with head and neck squamous cancer progression and administration of anti-PD-L1 antibodies inhibits the immunosuppressive function of PD-L1 (53). PD-L1 is a ligand for PD-1 on the surface of T cells; however, this review (53) presents no evidence about the relationship between exosomal PD-L1 and T cell activity. Another study reported that genetic blockage of exosomal PD-L1 promoted T cell activity in the draining lymph node to induce systemic antitumor immunity and memory (44). The aforementioned study (44) directly identified the inhibitory effect of exosome PD-L1 on T cell activity, but GDLBCL was not involved. In comparison, the present study demonstrated the suppression of exosomal PD-L1 on T-cell activation in GDLBCL, which indicated the significance of exosomal PD-L1 in the formation of an immunosuppressive microenvironment.

The present study demonstrated the prognostic role of PD-L1 in plasma exosomes in GDLBCL and analyzed the association between the protein expression level of exosomal PD-L1 and the immune microenvironment, which highlighted the importance of exosomal PD-L1 in the development and immune evasion of GDLBCL. The significance and innovations of the present study were as follows: Firstly, high expression of exosomal PD-L1 was demonstrated to be positively related with the malignant transformation and poor prognosis of GDLBCL. Secondly, the upregulated expression of PD-L1 in plasma exosomes was identified as a potential indicator for the immunosuppressive microenvironment of GDLBCL. The present study further demonstrated the significance of the PD-1/PD-L1 axis in the development and therapy of GDLBCL and indicated the possibility of exosomal PD-L1 as a predictor of clinical anti-PD-1 immunotherapy.

Acknowledgements

Not applicable.

Funding

This study was financially supported by the National Natural Science Foundation of China (grant no. 82170192).

Availability of data and materials

The datasets used and/or analyzed during the present study are available from the corresponding author upon reasonable request.

Authors' contributions

CZ and YL conceived and designed the experiments. HZe, JW, BX and HD performed the main experiments and analyzed the data. MP, RD and SS collected tissue and blood samples. QH established the cell lines. JLi and JLin conducted the protein experiments. HZh helped to design the experiments. YL and CZ wrote the manuscript. RD and HZh performed language correction. HZe, CZ and YL confirm the authenticity of all the raw data. All authors have read and approved the final manuscript.

Ethics approval and consent to participate

All tissue specimens used in this study were obtained from Hunan Cancer Hospital with informed consent from patients and the present study was approved by the institutional review boards of Hunan Cancer Hospital (approval no. 2021-012) and in accordance with the Declaration of Helsinki.

Animal experiments were approved by the Animal Care and Experiment Committee of Hunan Cancer Hospital (approval no. SBQLL-2021-050). All procedures performed in the experiments were in accordance with the Animal Care and Experiment Committee of Hunan Cancer Hospital.

Patient consent for publication

Not applicable.

Competing interests

The authors declare that they have no competing interests.

References

- Juarez-Salcedo LM, Sokol L, Chavez JC and Dalia S: Primary gastric lymphoma, epidemiology, clinical diagnosis, and treatment. *Cancer Control* 25: 1073274818778256, 2018.
- Fujishima F, Katsushima H, Fukuhara N, Konosu-Fukaya S, Nakamura Y, Sasano H and Ichinohasama R: Incidence rate, subtype frequency, and occurrence site of malignant lymphoma in the gastrointestinal tract: Population-based analysis in miyagi, Japan. *Tohoku J Exp Med* 245: 159-165, 2018.
- Rotaru I, Găman GD, Stănescu C and Găman AM: Evaluation of parameters with potential prognosis impact in patients with primary gastric diffuse large B-cell lymphoma (PG-DLBCL). *Rom J Morphol Embryol* 55: 15-21, 2014.
- Deng Y, Su W, Zhu J, Ji H, Zhou X, Geng J, Zhu J and Zhang Q: *Helicobacter pylori* infection disturbs the tumor immune micro-environment and is associated with a discrepant prognosis in gastric de novo diffuse large B-cell lymphoma. *J Immunother Cancer* 9: e002947, 2021.
- Zepeda-Gomez S, Camacho J, Oviedo-Cardenas E and Lome-Maldonado C: Gastric infiltration of diffuse large B-cell lymphoma: endoscopic diagnosis and improvement of lesions after chemotherapy. *World J Gastroenterol* 14: 4407-4409, 2008.
- Topalian SL, Drake CG and Pardoll DM: Immune checkpoint blockade: A common denominator approach to cancer therapy. *Cancer Cell* 27: 450-461, 2015.
- Ansell SM, Lesokhin AM, Borrello I, Halwani A, Scott EC, Gutierrez M, Schuster SJ, Millenson MM, Cattray D, Freeman GJ, *et al*: PD-1 blockade with nivolumab in relapsed or refractory Hodgkin's lymphoma. *N Engl J Med* 372: 311-319, 2015.
- Schumacher TN, Kesmir C and van Buuren MM: Biomarkers in cancer immunotherapy. *Cancer Cell* 27: 12-14, 2015.
- Sia D, Jiao Y, Martinez-Quetglas I, Kuchuk O, Villacorta-Martin C, Castro de Moura M, Putra J, Camprecios G, Bassaganyas L, Akers N, *et al*: Identification of an Immune-specific Class of Hepatocellular Carcinoma, Based on Molecular Features. *Gastroenterology* 153: 812-826, 2017.
- Li CJ, Lin LT, Hou MF and Chu PY: PDL1/PD1 blockade in breast cancer: The immunotherapy era (Review). *Oncol Rep* 45: 5-12, 2021.
- Sohn BS, Kim SM, Yoon DH, Kim S, Lee DH, Kim JH, Lee SW, Huh J and Suh C: The comparison between CHOP and R-CHOP in primary gastric diffuse large B cell lymphoma. *Ann Hematol* 91: 1731-1739, 2012.
- Deng R, Zuo C, Li Y, Xue B, Xun Z, Guo Y, Wang X, Xu Y, Tian R, Chen S, *et al*: The innate immune effector ISG12a promotes cancer immunity by suppressing the canonical Wnt/ β -catenin signaling pathway. *Cell Mol Immunol* 17: 1163-1179, 2020.
- Wang J, Shang S, Li J, Deng H, Ouyang L, Xie H, Zhu H, Li Y and Zuo C: PD-L1 and miR-34a are prognostic factors for primary gastric diffuse large B-cell lymphoma patients treated with R-CHOP. *Cancer Manag Res* 12: 4999-5008, 2020.
- van Niel G, D'Angelo G and Raposo G: Shedding light on the cell biology of extracellular vesicles. *Nat Rev Mol Cell Biol* 19: 213-228, 2018.
- Shao H, Im H, Castro CM, Breakefield X, Weissleder R and Lee H: New technologies for analysis of extracellular vesicles. *Chem Rev* 118: 1917-1950, 2018.
- Lobb RJ, Hastie ML, Norris EL, van Amerongen R, Gorman JJ and Moller A: Oncogenic transformation of lung cells results in distinct exosome protein profile similar to the cell of origin. *Proteomics* 17: 1600432, 2017.
- Meehan K and Vella LJ: The contribution of tumour-derived exosomes to the hallmarks of cancer. *Crit Rev Clin Lab Sci* 53: 121-131, 2016.
- Moller A and Lobb RJ: The evolving translational potential of small extracellular vesicles in cancer. *Nat Rev Cancer* 20: 697-709, 2020.
- Nakaoka A, Nakahana M, Inubushi S, Akasaka H, Salah M, Fujita Y, Kubota H, Hassan M, Nishikawa R, Mukumoto N, *et al*: Exosome-mediated radiosensitizing effect on neighboring cancer cells via increase in intracellular levels of reactive oxygen species. *Oncol Rep* 45: 13, 2021.
- Theodoraki MN, Yerneni SS, Hoffmann TK, Gooding WE and Whiteside TL: Clinical significance of PD-L1⁺ exosomes in plasma of head and neck cancer patients. *Clin Cancer Res* 24: 896-905, 2018.
- Chen G, Huang AC, Zhang W, Zhang G, Wu M, Xu W, Yu Z, Yang J, Wang B, Sun H, *et al*: Exosomal PD-L1 contributes to immunosuppression and is associated with anti-PD-1 response. *Nature* 560: 382-386, 2018.
- Sun Y, Guo J, Yu L, Guo T, Wang J, Wang X and Chen Y: PD-L1⁺ exosomes from bone marrow-derived cells of tumor-bearing mice inhibit antitumor immunity. *Cell Mol Immunol* 18: 2402-2409, 2021.
- Chen Z, You L, Wang L, Huang X, Liu H, Wei JY, Zhu L and Qian W: Dual effect of DLBCL-derived EXOs in lymphoma to improve DC vaccine efficacy in vitro while favor tumorigenesis in vivo. *J Exp Clin Cancer Res* 37: 190, 2018.
- Saibil SD and Ohashi PS: Targeting T cell activation in immuno-oncology. *Curr Oncol* 27 (Suppl 2): S98-S105, 2020.
- Chen DS and Mellman I: Elements of cancer immunity and the cancer-immune set point. *Nature* 541: 321-330, 2017.
- El-Galaly TC, Cheah CY, Kristensen D, Hutchison A, Hay K, Callreus T and Villa D: Potentials, challenges and future of chimeric antigen receptor T-cell therapy in non-Hodgkin lymphomas. *Acta Oncol* 59: 766-774, 2020.
- Wang T, Xu L, Gao L, Tang G, Chen L, Chen J, Wang Y, Fu W, Yue W, Ye M, *et al*: Chimeric antigen receptor T-cell therapy combined with autologous stem cell transplantation improved progression-free survival of relapsed or refractory diffuse large B-cell lymphoma patients: A single-center, retrospective, cohort study. *Hematol Oncol* 40: 637-644, 2022.
- Thery C, Amigorena S, Raposo G and Clayton A: Isolation and characterization of exosomes from cell culture supernatants and biological fluids. *Curr Protoc Cell Biol*: Chapter 3:Unit 3.22, 2006.
- Shang S, Wang J, Chen S, Tian R, Zeng H, Wang L, Xia M, Zhu H and Zuo C: Exosomal miRNA-1231 derived from bone marrow mesenchymal stem cells inhibits the activity of pancreatic cancer. *Cancer Med* 8: 7728-7740, 2019.
- Cheson BD, Ansell S, Schwartz L, Gordon LI, Advani R, Jacene HA, Hoos A, Barrington SF and Armand P: Refinement of the lugano classification lymphoma response criteria in the era of immunomodulatory therapy. *Blood* 128: 2489-2496, 2016.
- Sehn LH, Berry B, Chhanabhai M, Fitzgerald C, Gill K, Hoskins P, Klasa R, Savage KJ, Shenker T, Sutherland J, *et al*: The revised International Prognostic Index (R-IPI) is a better predictor of outcome than the standard IPI for patients with diffuse large B-cell lymphoma treated with R-CHOP. *Blood* 109: 1857-1861, 2007.
- Malipatel R, Patil M, Pritilata Rout P, Correa M and Devarbhavi H: Primary Gastric Lymphoma: Clinicopathological Profile. *Euroasian J Hepatogastroenterol* 8: 6-10, 2018.
- Brahmer JR, Tykodi SS, Chow LQ, Hwu WJ, Topalian SL, Hwu P, Drake CG, Camacho LH, Kauh J, Odunsi K, *et al*: Safety and activity of anti-PD-L1 antibody in patients with advanced cancer. *N Engl J Med* 366: 2455-2465, 2012.
- Postow MA, Callahan MK and Wolchok JD: Immune Checkpoint Blockade in Cancer Therapy. *J Clin Oncol* 33: 1974-1982, 2015.
- Page DB, Postow MA, Callahan MK, Allison JP and Wolchok JD: Immune modulation in cancer with antibodies. *Annu Rev Med* 65: 185-202, 2014.
- Wei Y, Zhao Q, Gao Z, Lao XM, Lin WM, Chen DP, Mu M, Huang CX, Liu ZY, Li B, *et al*: The local immune landscape determines tumor PD-L1 heterogeneity and sensitivity to therapy. *J Clin Invest* 129: 3347-3360, 2019.
- You W, Shang B, Sun J, Liu X, Su L and Jiang S: Mechanistic insight of predictive biomarkers for antitumor PD1/PDL1 blockade: A paradigm shift towards immunome evaluation (Review). *Oncol Rep* 44: 424-437, 2020.
- Juneja VR, McGuire KA, Manguso RT, LaFleur MW, Collins N, Haining WN, Freeman GJ and Sharpe AH: PD-L1 on tumor cells is sufficient for immune evasion in immunogenic tumors and inhibits CD8 T cell cytotoxicity. *J Exp Med* 214: 895-904, 2017.
- Chen BJ, Chapuy B, Ouyang J, Sun HH, Roemer MG, Xu ML, Yu H, Fletcher CD, Freeman GJ, Shipp MA and Rodig SJ: PD-L1 expression is characteristic of a subset of aggressive B-cell lymphomas and virus-associated malignancies. *Clin Cancer Res* 19: 3462-3473, 2013.
- Tanaka A and Sakaguchi S: Regulatory T cells in cancer immunotherapy. *Cell Res* 27: 109-118, 2017.

41. Groth C, Hu X, Weber R, Fleming V, Altevogt P, Utikal J and Umansky V: Immunosuppression mediated by myeloid-derived suppressor cells (MDSCs) during tumour progression. *Br J Cancer* 120: 16-25, 2019.
42. Boussiotis VA: Molecular and biochemical aspects of the PD-1 checkpoint pathway. *N Engl J Med* 375: 1767-1778, 2016.
43. Bunggulawa EJ, Wang W, Yin T, Wang N, Durkan C, Wang Y and Wang G: Recent advancements in the use of exosomes as drug delivery systems. *J Nanobiotechnology* 16: 81, 2018.
44. Poggio M, Hu T, Pai CC, Chu B, Belair CD, Chang A, Montabana E, Lang UE, Fu Q, Fong L and Blelloch R: Suppression of exosomal PD-L1 induces systemic anti-tumor immunity and memory. *Cell* 177: 414-427.e13, 2019.
45. Daassi D, Mahoney KM and Freeman GJ: The importance of exosomal PDL1 in tumour immune evasion. *Nat Rev Immunol* 20: 209-215, 2020.
46. Wen SW, Sceneay J, Lima LG, Wong CS, Becker M, Krumeich S, Lobb RJ, Castillo V, Wong KN, Ellis S, *et al*: The biodistribution and immune suppressive effects of breast cancer-derived exosomes. *Cancer Res* 76: 6816-6827, 2016.
47. Morrissey SM and Yan J: Exosomal PD-L1: Roles in tumor progression and immunotherapy. *Trends Cancer* 6: 550-558, 2020.
48. Sharma P, Diergaarde B, Ferrone S, Kirkwood JM and Whiteside TL: Melanoma cell-derived exosomes in plasma of melanoma patients suppress functions of immune effector cells. *Sci Rep* 10: 92, 2020.
49. Wu L, Zhang X, Zhang B, Shi H, Yuan X, Sun Y, Pan Z, Qian H and Xu W: Exosomes derived from gastric cancer cells activate NF- κ B pathway in macrophages to promote cancer progression. *Tumour Biol* 37: 12169-12180, 2016.
50. Gabrusiewicz K, Li X, Wei J, Hashimoto Y, Marisetty AL, Ott M, Wang F, Hawke D, Yu J, Healy LM, *et al*: Glioblastoma stem cell-derived exosomes induce M2 macrophages and PD-L1 expression on human monocytes. *Oncoimmunology* 7: e1412909, 2018.
51. Andorsky DJ, Yamada RE, Said J, Pinkus GS, Betting DJ and Timmerman JM: Programmed death ligand 1 is expressed by non-hodgkin lymphomas and inhibits the activity of tumor-associated T cells. *Clin Cancer Res* 17: 4232-4244, 2011.
52. Rossille D, Gressier M, Damotte D, Maucourt-Boulch D, Pangault C, Semana G, Le Gouill S, Haioun C, Tarte K, Lamy T, *et al*: High level of soluble programmed cell death ligand 1 in blood impacts overall survival in aggressive diffuse large B-Cell lymphoma: Results from a French multicenter clinical trial. *Leukemia* 28: 2367-2375, 2014.
53. Sinha D, Roy S, Saha P, Chatterjee N and Bishayee A: Trends in research on exosomes in cancer progression and anticancer therapy. *Cancers (Basel)* 13: 326, 2021.



This work is licensed under a Creative Commons Attribution-NonCommercial-NoDerivatives 4.0 International (CC BY-NC-ND 4.0) License.